Journal of Electron Devices, Vol. 7, 2010, pp. 235-240

© JED [ISSN: 1682 -3427]

Journal of Electron Devices
www.jeldev.org

Linear Profile Based Analytical Surface Potential Model For Pocket Implanted Sub-100 nm n-MOSFET

Muhibul Haque Bhuyan[1,2] and Quazi D. M. Khosru[2]
[1]Department of Electrical and Electronic Engineering
Daffodil International University, Dhaka, Bangladesh
[2]Department of Electrical and Electronic Engineering
Bangladesh University of Engineering and Technology, Dhaka, Bangladesh
E-mail: muhibulhb@gmail.com

Received 3 March 2010

Abstract: *This paper presents an analytical surface potential model for pocket implanted sub-100 nm n-MOSFET. The model is derived by solving the Poisson's equation in the depletion region at the surface with the appropriate boundary conditions at source and drain. The model includes the effective doping concentration of the two linear pocket profiles at the source and drain sides of the device. The model also incorporates the drain and substrate bias effect below and above threshold conditions. The simulation results show that the derived surface potential model has a simple compact form that can be utilized to study and characterize the pocket implanted advanced ULSI devices.*

Keywords: *Linear pocket profile, pocket implantation, n-MOSFET, threshold voltage, surface potential, short channel effect (SCE), reverse short channel effect (RSCE).*

1. INTRODUCTION

As the channel length of MOSFETs is scaled down to deep-submicrometer or sub-100 nm regime, we observe the reduction of threshold voltage with the reduction of channel length due to the charge sharing between the drain/source region and the channel [1]. Also, the off-state leakage current increases due to sensitivity of the source/channel barrier to the drain potential or drain induced barrier lowering (DIBL). This effect is known as short-channel effect (SCE). This effect arises as a result of two dimensional potential distribution and high electric fields in the channel region [2]. It can be reduced or can be even reversed (then it is called reverse short channel effect or RSCE) by locally raising the channel doping near source and drain junctions. RSCE was originally observed in MOSFETs due to oxidation-enhanced-diffusion [3] or implant-damage-enhanced diffusion [4] which are very difficult to control. Lateral channel engineering utilizing halo or pocket implant [5-9] surrounding drain and source regions is effective in suppressing short channel effects. The halo or pocket implant can be either symmetrical [10] or asymmetrical [11] with respect to source or drain. Reported circuit applications include a 256 M-bit DRAM [12] and mixed-signal processor [13]. In fact, this pocket implant technology is found to be very promising in the effort to tailor the short-channel performances of deep-submicron as well as sub-100 nm MOSFETs although careful tradeoffs need to be made between minimum channel length and other device electrical parameters [6].

Solution of the Poisson's equation in the depletion region of the MOSFETs is an important step in order to determine the surface potential. Numerical device simulators like MEDICI [14] can produce most accurate solutions of the Poisson's equation. But analytical models that have been used for MOSFET device design, take less time for device simulation. It also provides device physics insight [15]. Analytical model shown in [6] does not satisfy the boundary conditions and device simulation results of MEDICI. Analytical model in [15] assume a step profile of pocket doping. Besides, Gaussian profile [16] and hyperbolic cosine function [17] were assumed for the pocket profile to derive the threshold voltage equations. But it has been observed that linear profile of pocket doping produce better results for threshold voltage [18]. The previous works [15-18] are on the threshold voltage modelling of pocket implanted MOS devices.

In this paper, an analytical model that can predict the surface potential of the sub-100 nm pocket implanted n-MOSFET is derived assuming the linear profile of pocket doping. Here the 1-D pocket profile across the channel has been transformed to an effective doping concentration expression, which is used in the Gauss's law to derive the model applying the appropriate boundary conditions at the source and drain. Simulation results show that the model predicts surface potential very well for various device and pocket profile parameters as well as various bias conditions, and also satisfies the boundary conditions. Comparison with other pocket profiles also shows the improvement of minimum surface potential. It proves the validity and usefulness of our proposed model for circuit simulation of next generation ULSI devices.

2. POCKET DOPING PROFILE

The pocket implanted n-MOSFET structure shown in Fig. 1 is considered in this work and assumed co-ordinate system is shown at the right side of the structure.

All the device dimensions are measured from the oxide-silicon interface. In the structure, the junction depth (r_j) is 25 nm. The oxide thickness (t_{ox}) is 2.5 nm, and it is SiO_2 with fixed oxide charge density of 10^{11} cm^{-2}. Uniformly doped p-type Si substrate is used with doping concentration (N_{sub}) of 4.2×10^{17} cm^{-3} with pocket implantation both at the source and drain side with peak pocket doping concentration of 1.5×10^{18} cm^{-3} and pocket lengths from 20 to 30 nm, and source or drain doping concentration of 9.0×10^{20} cm^{-3}.

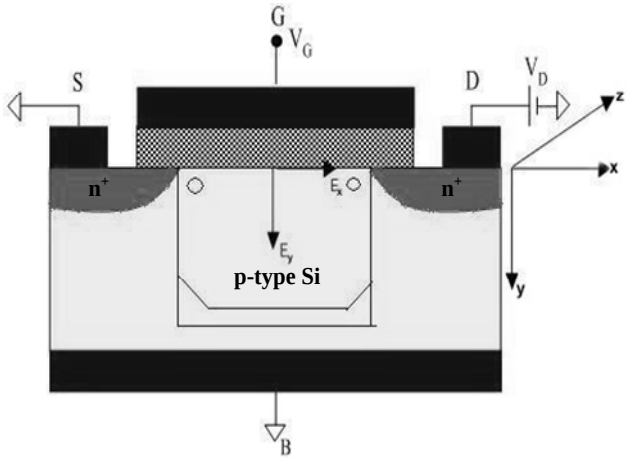

Fig. 1 Pocket implanted n-MOSFET Structure

The model of the conventional bulk n-MOSFET exhibits drastic reduction of the threshold voltage (ΔV_{th}) from the long channel value beyond 100 nm. This is known as short channel effect. A group of analytical models, known as "charge-sharing" models, are found in the literature. But their accuracy is limited [12]. In [12], a model is presented that solves the two-dimensional Poisson equation analytically, and predicts threshold voltage change (ΔV_{th}) accurately as a function of drain bias (V_D), substrate bias (V_{BS}), channel length (L), oxide thickness (t_{ox}) and substrate concentration (N_{sub}). This model is then transformed to short channel n-MOSFET assuming the step doping profile along the vertical direction of the channel.

To preserve the long channel threshold voltage behavior for the short channel device, pocket implantation, which causes reverse short channel effect (RSCE), is done by adding acceptor atoms both from the source and drain edges. The peak pocket doping concentration (N_{pm}) gradually decreases towards the substrate level concentration (N_{sub}) with pocket length (L_p) from both the source and drain edges. The basis of the model of the pocket is to assume two laterally linear doping profiles from both the source and drain edges across the channel as shown in Figs. 2-3 for substrate concentration of 4.2×10^{17} cm^{-3} and channel length of 100 nm. The pocket parameters, N_{pm} and L_p, play important role in determining the RSCE.

At the source side, the pocket profile is given as:

$$N_s(x) = -\frac{N_{pm} - N_{sub}}{L_p}x + N_{pm}$$

$$N_s(x) = N_{sub}\frac{x}{L_p} + N_{pm}\left(1 - \frac{1}{L_p}x\right) \quad (1)$$

At the drain side, the pocket profile is given as:

$$N_d(x) = \frac{N_{pm} - N_{sub}}{L_p}\left[x - \left(L - L_p\right)\right] + N_{sub}$$

$$N_d(x) = N_{sub}\left(\frac{L}{L_p} - \frac{1}{L_p}x\right) + N_{pm}\left(1 - \frac{L}{L_p} + \frac{1}{L_p}x\right) \quad (2)$$

where x represents the distance across the channel. Since these pile-up profiles are due to the direct pocket implantation at the source and drain sides, the pocket profiles are assumed symmetric at both sides.

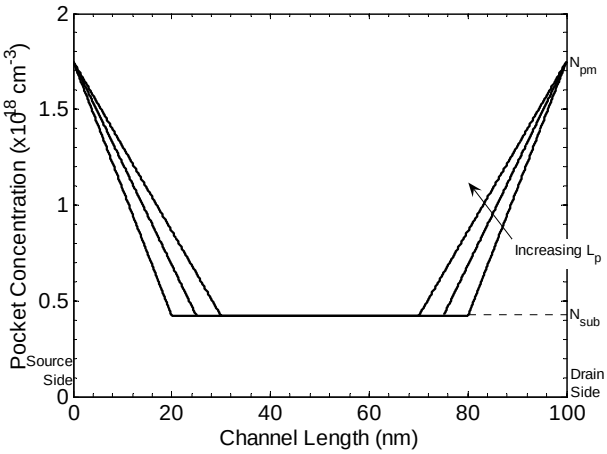

Fig. 2 Simulated pocket profiles at the surface for different pocket lengths, L_p = 20, 25 and 30 nm; peak pocket concentration, $N_{pm} = 1.75\times10^{18}$ cm^{-3}

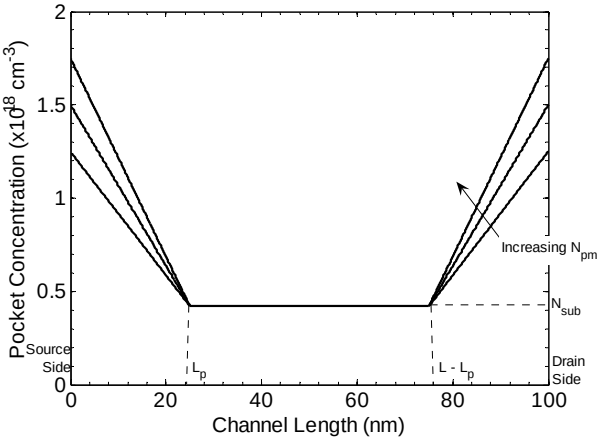

Fig. 3 Simulated pocket profiles at the surface for various peak pocket concentrations, $N_{pm} = 1.25\times10^{18}$, 1.5×10^{18} and 1.75×10^{18} cm^{-3}; pocket length, L_p = 25 nm

With these two conceptual pocket profiles, the profiles

are integrated mathematically along the channel length and then divided by it to derive an average effective doping concentration (N_{eff}) as in equation (3).

$$N_{eff} = \frac{1}{L}\int_0^L \left[N_s(x) + N_d(x) + N_{sub} \right] dx \qquad (3)$$

Putting the expressions of $N_s(x)$ and $N_d(x)$ from equations (1) and (2) in equation (3) the effective doping concentration is obtained in equation (4).

$$N_{eff} = N_{sub}\left(1 - \frac{L_p}{L}\right) + \frac{N_{pm} L_p}{L} \qquad (4)$$

This effective doping concentration expression will be used in deriving the surface potential model by applying Gauss's law. When $L_p << L$ for long channel device then the pocket profile has very little effect on uniform substrate concentration, but when L_p is comparable with L then the pocket profile parameters affects the substrate doping concentration at the surface of the n-MOSFET. This causes the surface potential to change and hence the threshold voltage (V_{th}).

3. SURFACE POTENTIAL MODEL

In the region under the gate oxide and at the surface of the MOS device, a negatively charged depletion layer is created when gate bias is applied. In this region, by applying Gauss's law and incorporating the effect of substrate bias and effective doping concentration along the channel as obtained in equation (4), we can write equation (5).

$$\varepsilon_s \frac{X_D}{\eta}\frac{dE}{dx} + \varepsilon_{ox}\frac{V_{GS} - V_{BS} - V_{FB} - \psi_s(x)}{t_{ox}} = qN_{eff} X_D \qquad (5)$$

where E, ε_s, ε_{ox}, V_{GS}, V_{BS}, V_{FB}, $\psi_s(x)$, t_{ox} and q is are the electric field, dielectric permittivity of Si and oxide, gate and substrate bias, flat band voltage, surface potential, oxide thickness and electronic charge. η is a fitting parameter, and it is assumed 1 everywhere. The depletion layer thickness, X_D is given by the expression as given in equation (6).

$$X_D = \sqrt{\frac{2\varepsilon_s(\varphi_F - V_{BS})}{qN_{eff}}} \qquad (6)$$

where φ_F is the Fermi potential due to pocket implantation as well as substrate doping concentration and is given as follows

$$\varphi_F = \frac{kT}{q}\ln\frac{N_{eff}}{n_i} \qquad (7)$$

The lateral electric field is defined as

$$E = \frac{d\psi_s(x)}{dx} \qquad (8)$$

Therefore, from equation (5) we can write

$$\varepsilon_s \frac{X_D}{\eta}\frac{d^2\psi_s(x)}{dx^2} + \varepsilon_{ox}\frac{V_{GS} - V_{BS} - V_{FB} - \psi_s(x)}{t_{ox}} = qN_{eff} X_D \qquad (9)$$

Now we assume the following boundary conditions:
1. At $x = 0$, i.e. at the source side, the surface potential is $\psi_s(0) = \varphi_{bi} - V_{BS}$.
2. At $x = L$, i.e. at the drain end, the surface potential is $\psi_s(L) = \varphi_{bi} - V_{BS} + V_{DS}$.

After solving the 2nd order differential equation of (9) using the above two boundary conditions we get the desired complete analytical expression for the surface potential as follows

$$\psi_s(x) = \frac{c_1}{\sinh\sqrt{\frac{a_0}{a_2}}L}\sinh\sqrt{\frac{a_0}{a_2}}(L - x) + \frac{c_1 + V_{DS}}{\sinh\sqrt{\frac{a_0}{a_2}}L}\sinh\sqrt{\frac{a_0}{a_2}}x - \frac{b_1}{a_0} \qquad (10)$$

where the parameters a_0, a_2, b_1 and c_1 are given by the following expressions (11)-(13).

$$a_0 = \frac{\varepsilon_{ox}}{t_{ox}}, \quad a_2 = \frac{\varepsilon_s}{\eta} X_D \qquad (11)$$

$$b_1 = qN_{eff} X_D - \frac{\varepsilon_{ox}}{t_{ox}}(V_{GS} - V_{BS} - V_{FB}) \qquad (12)$$

$$c_1 = \varphi_{bi} - V_{BS} + \frac{b_1}{a_0} \qquad (13)$$

The complete solution is obtained by finding the transient solution and the particular integral using the conventional differential equation solution techniques and then adding the two solutions together.

4. RESULTS AND DISCUSSION

In order to verify the derived analytical surface potential model for the pocket implanted n-MOSFET, different types of simulations were performed. At first, the bias conditions are changed and then the device parameters and pocket profile parameters are changed to verify our proposed model. Then a comparison is made with the other pocket profile models.

Figure 4 shows the variation of surface potential along the channel for different drain biases. It has been observed that as the drain bias increases surface potential

increases at the drain side whereas it remains constant at the source side. It proves the validity of our assumed boundary conditions while deriving the model.

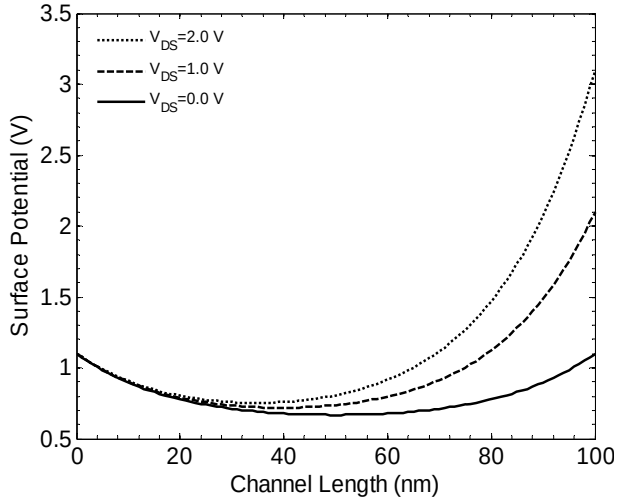

Fig. 4 Surface potential vs. channel length curves for various drain biases with channel length, L = 100 nm and substrate bias, V_{BS} = 0.0 V

From Fig. 5, it is observed that as the substrate bias increases in the negative direction keeping drain bias constant at 0 V, both sides of the curve shifts upward. Since when the substrate bias increases depletion charge increases thereby increasing the surface potential.

Figure 6 shows the variation of surface potential along the channel for different gate voltages below the threshold voltage with channel length of 0.1 μm. It is observed from this figure that as the gate voltage is increased the peak of potential minimum shifts upward without changing the boundary values. The reason for increase of the surface potential can be attributed to the increase of the depletion layer charge with the gate bias.

From Fig. 7, it is found that as the channel lengths are decreased from 100 nm to 50 nm the surface potential is same as in Fig. 4 for V_{DS} = 1.0 V at both sides of the device. But the potential minimum shifts upward direction as the channel lengths are decreased. This occurs due to the widening of the depletion region under the gate at the surface.

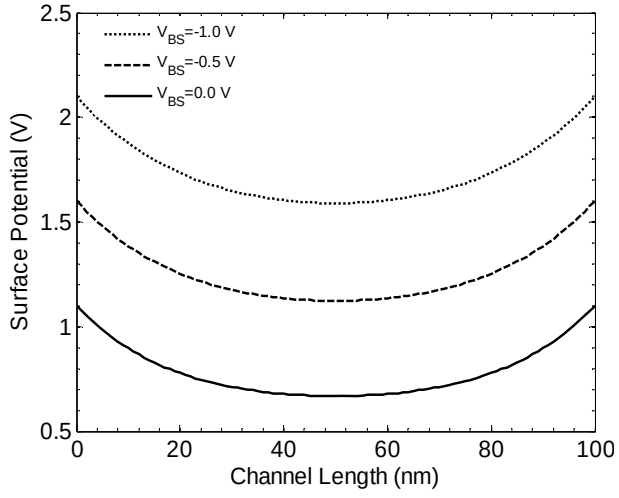

Fig. 5 Surface potential vs. channel length curves for various substrate biases with channel length, L = 100 nm and drain bias, VDS = 0.0 V

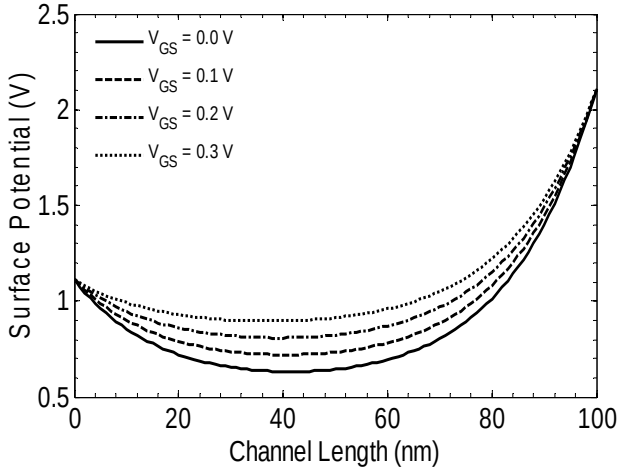

Fig. 6 Surface potential curves along the channel for various gate biases below the threshold voltage with channel length, L = 100 nm, substrate bias, V_{BS} = 0.0 V and drain bias, V_{DS} = 1.0 V

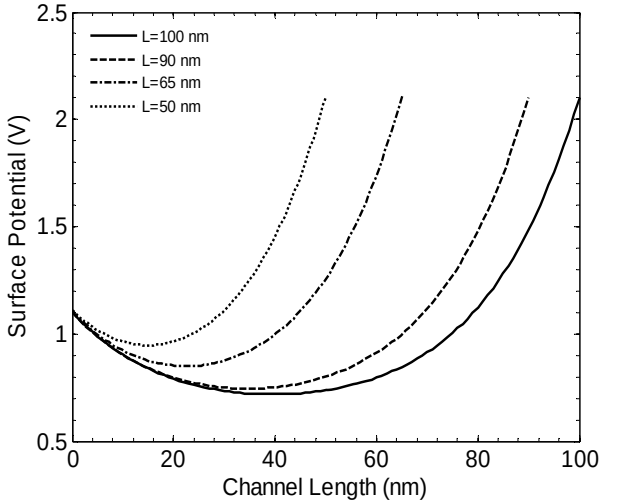

Fig. 7 Surface potential curves along the channel for various channel lengths with substrate bias, V_{BS} = 0.0 V and drain bias, V_{DS} = 1.0 V

Figure 8 shows the variation of surface potential along the channel for different oxide thicknesses with zero substrate bias and drain bias, V_{DS} = 1.0 V. It is observed that as the oxide thickness decreases the potential minimum increases near the source side. But near the drain, opposite phenomenon is observed. When oxide thickness decreases oxide capacitance increases. This increases the surface charge and hence surface potential for a fixed bias condition. Since at the drain side with the reduction of the oxide thickness, the oxide capacitance increases as well as the off-state current increases thus the potential at the drain side decreases. Hence DIBL effect will be more pronounced as the oxide thickness is decreased at the drain side.

Figure 9 shows that the surface potential increases with the decreasing pocket lengths. Since when the pocket length decreases the effective doping concentration also

decreases and thus depletion charge decreases. But the boundary value remains the same as expected.

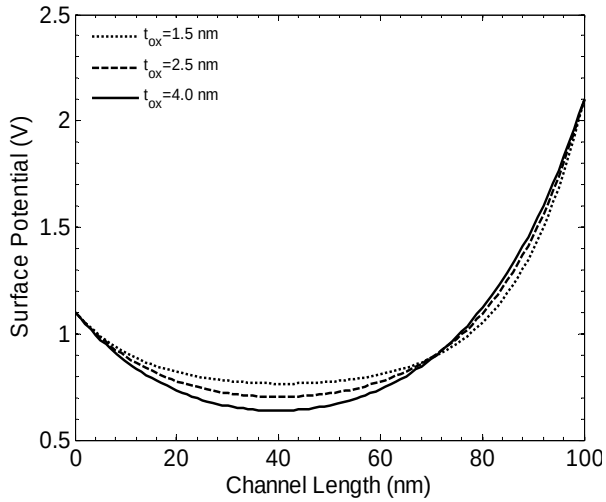

Fig. 8 Surface potential curves along the channel for various oxide thicknesses with channel length, L = 100 nm, substrate bias, V_{BS} = 0.0 V and drain bias, V_{DS} = 1.0 V

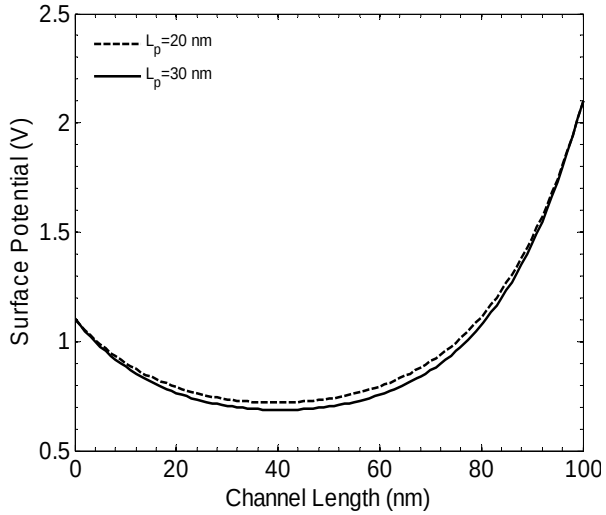

Fig. 9 Surface potential curves along the channel for various pocket lengths with channel length, L = 100 nm, substrate bias, V_{BS} = 0.0 V and drain bias, V_{DS} = 1.0 V

Figure 10 shows the surface potential variation with the position of the channel for different peak pocket doping concentration. It is observed that the surface potential increases as the peak pocket doping concentration increases. This is due to the increase of effective carrier concentration along the channel. The results are shown for zero substrate bias and drain bias of 1 V.

Figure 11 shows the surface potential curves along the channel for our linear profiles with two other pocket doping profile models found in the literature, such as, Gaussian function [16] and hyperbolic cosine function [17] models. These two pocket doping models are used in our analytical surface potential model and then simulated for various bias conditions and pocket profiles and device parameters. It is found that the proposed model works well and satisfies all the conditions of the surface potential model found in various literatures.

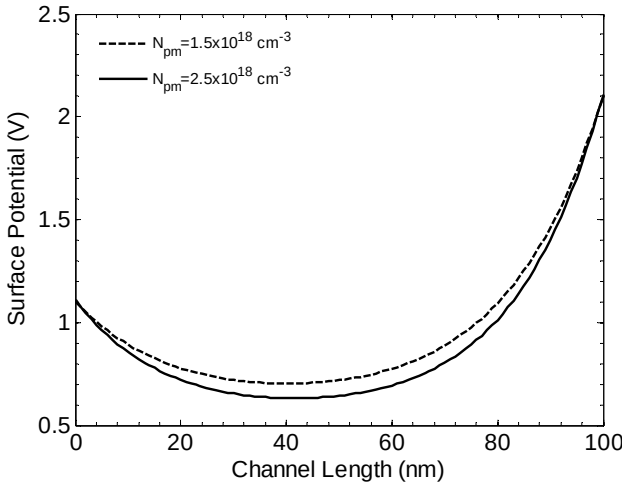

Fig. 10 Surface potential curves along the channel for various peak pocket doping concentration with channel length, L = 100 nm, substrate bias, V_{BS} = 0.0 V and drain bias, V_{DS} = 1.0 V

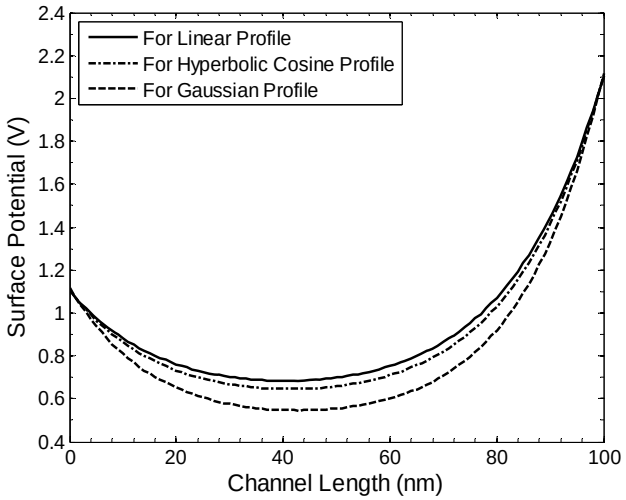

Fig. 11 Surface potential curves along the channel for various pocket profiles found in the literature with channel length, L = 100 nm, substrate bias, V_{BS} = 0.0 V, drain bias, V_{DS} = 1.0 V and pocket length, L_p = 25 nm

5. CONCLUSION

An analytical surface model for ultra thin oxide and sub-100 nm pocket implanted n-MOSFET has been developed incorporating the substrate and drain bias dependence. The model is developed assuming two linear pocket profiles along the channel at the surface of the MOS device from the source and drain edges. The effect of changing the device and pocket profiles parameters on the surface potential have been studied using the proposed model. The simulated results show that the proposed model satisfies the boundary conditions as well as predicts the surface potential down to 50 nm channel length. Besides, comparison of two other pocket profiles with our proposed model shows the satisfactory behavior of our model. It shows the expected results when the various parameters are changed. Hence this model efficiently determines the surface potential of scaled pocket n-MOSFETs having channel lengths in sub-100 nm regime.

REFERENCES

[1] S. M. Sze, "Physics of Semiconductor Devices," 2nd Edition, John Wiley & Sons, New York, ch. 8, (1981).

[2] M. Miura-Mattausch, M. Suetake, H. J. Mattausch, S. Kumashiro, N. Shigyo, S. Oganaka and N. Nakayama, "Physical modeling of the reverse short channel effect for circuit simulation," IEEE Transactions on Electron Devices, 48, 2449-2452, (2001).

[3] M. Orlowski, C. Mazure and F. Lau, "Submicron short channel effects due to gate reoxidation induced lateral interstitial diffusion," IEEE IEDM Technical Digest, 632, (1987).

[4] M. Nishida and H. Onodera, "An anomalous increase of threshold voltage with shortening the channel lengths for deeply boron-implanted n-channel MOSFETs," IEEE Transactions on Electron Devices, 48, 1101, (1981).

[5] K. Y. Lim and X. Zhou, "Modeling of Threshold Voltage with Non-uniform Substrate Doping," in Proc. of the IEEE International Conference on Semiconductor Electronics (ICSE'98), Malaysia, 27-31, (1998).

[6] B. Yu, C. H. Wann, E. D. Nowak, K. Noda and C. Hu, "Short Channel Effect improved by lateral channel engineering in deep-submicrometer MOSFETs," IEEE Transactions on Electron Devices, 44, 627-633, (1997).

[7] B. Yu, H. Wang, O. Millic, Q. Xiang, W. Wang, J. X. An and M. R. Lin, "50 nm gate length CMOS transistor with super-halo: Design, process and reliability," IEDM Technical Digest, 653-656, (1999).

[8] K. M. Cao, W. Liu, X. Jin, K. Vasant, K. Green, J. Krick, T. Vrotsos and C. Hu, "Modelling of pocket implanted MOSFETs for anomalous analog behavior," IEEE IEDM Technical Digest, 171-174, (1999).

[9] Y. S. Pang and J. R. Brews, "Models for subthreshold and above subthreshold currents in 0.1 μm pocket n-MOSFETs for low voltage applications," IEEE Transactions on Electron Devices, 49, 832-839, (2002).

[10] J. Tanaka, S. Kimura, H. Noda, T. Toyabe, and S. Ihara, "A sub-0.1 μm grooved gate MOSFET with high immunity to short channel effects," IEEE IEDM Technical Digest, 537, (1993).

[11] T. N. Buti, S. Ogura, N. Rovedo, K. Tobimatsu, and C. F. Codella, "Asymmetrical halo source GOLD drain (HS-GOLD) deep-half-micron n-MOSFET design for reliability and performance," IEEE IEDM Technical Digest, 617, (1989).

[12] A. Chatterjee, J. Liu, P. K. Mozumder, M. Rodder and I. C. Chen, "Pass transistor designs using pocket implant to improve manufacturability for 256-Mbit DRAM and beyond," IEEE IEDM Technical Digest, 87, (1994).

[13] H. Chen, J. Zhiao, C. S. Teng, L. Moberly and R. Lahri, "Submicron large-angle-tilt-implanted drain technology for mixed signal applications," IEEE IEDM Technical Digest, 91, (1994).

[14] "MEDICI ver. 1999.2," Avant! Corporation, Fremont, CA, USA, (1999).

[15] Y. S. Pang and J. R. Brews, "Analytical subthreshold surface potential model for pocket n-MOSFETs," IEEE Transactions on Electron Devices, 49, 2209-2216, (2002).

[16] X. Zhou, K. Y. Lim and D. Lim, "Physics-Based threshold voltage modeling with Reverse Short Channel Effect," Journal of Modeling and Simulation of Microsystems, 2, 1, 51-56, (1999).

[17] X. Zhou, K. Y. Lim and D. Lim, "A general approach to compact threshold voltage formulation based on 2-D numerical simulation and experimental correlation for deep-submicron ULSI technology development," IEEE Transactions on Electron Devices, 47, 1, 214-221, (2000).

[18] M. H. Bhuyan, F. Ferdous and Q. D. M. Khosru, "A threshold voltage model for sub-100 nm pocket implanted n-MOSFET," in Proc. of the 4th International Conference on Electrical and Computer Engineering (ICECE 2006), Dhaka, Bangladesh, 522-525, (2006).